Keck Adaptive Optics Note (KAON) 492:
Null-modes and quadratic mode tomography error in LGS-based multi-beacon tomography AO systems

Ralf Flicker (*rflicker@keck.hawaii.edu*)
Christopher Neyman (*cneyman@keck.hawaii.edu*)
W.M. Keck Observatory, 65-1120 Mamalahoa Hwy., Kamuela, HI 96743, USA

14 June 2007

Abstract

An overview of low-order errors in LGS-based multi-beacon tomography AO is given. The effects of tilt anisoplanatism and quadratic mode tomography error are analyzed separately, and compensation strategies evaluated numerically. Quadratic tomography error on-axis can be as large as 50 nm if insufficient NGS null-mode correction is supplied.

1   Introduction

A number of studies have given this phenomenon the treatment previously, such as e.g. Ellerbroek & Rigaut, 2001[2]; Flicker, Rigaut & Ellerbroek, 2003[4]; and Clare & Ellerbroek, 2006[1]. The analysis and results presented in this brief text is meant chiefly to complement those studies by clarifying some fundamental properties that are relevant to the NGAO design and architectural choices.

1.1   Overview

The employment of laser guide stars (LGS) for adaptive optics (AO) can offer a greater sky coverage than natural guide star (NGS) AO, but it comes at the expense of a focal anisoplanatism (cone effect) error. Furthermore, because of the tilt determination problem with LGS, the global tip and tilt (TT) modes must be filtered from LGS measurements: TT are forced to be "null-modes" of the LGS AO system (they map to the null space of the LGS interaction matrix). This leads to an additional tilt anisoplanatism error, induced by the necessity to use an off-axis NGS for TT compensation when the science target is not bright enough or too extended to be used itself for TT sensing. The cone effect error on an individual LGS can be countered by using multiple LGS and a tomographic wavefront reconstruction technique, in order to estimate the refractive index fluctuations in the volume probed by the beams. The fidelity of the tomographic estimation will be the highest where the beams overlap and the redundancy of WFS measurements is high. While a single LGS only has two null-modes that can be measured with a single TT NGS, the consequences of filtering TT from a multi-LGS tomography system are twofold:

1. Additional null-modes are created that produce off-axis tilt anisoplanatism. The null-modes depend on the geometry of the LGS asterism.

2. The estimation of quadratic modes from LGS will be biased by the cone effect, and produce an additional tomography error. This error is independent of the number and positions of LGS (see Sect. 1.2).

It should be pointed out that either or both of these effects could be (partly) solved by using LGS that provide TT information (e.g. polychromatic LGS), or by using LGS at different ranges (e.g. combining Sodium and Rayleigh beacons). The problem will be addressed here by instead allowing the NGS to measure and correct more modes.

The tilt anisoplanatism null-modes of item (1) can be visualized as combinations of modes with opposite signs occurring at different heights in the atmosphere. Their modal content are constructed such that all terms of quadratic
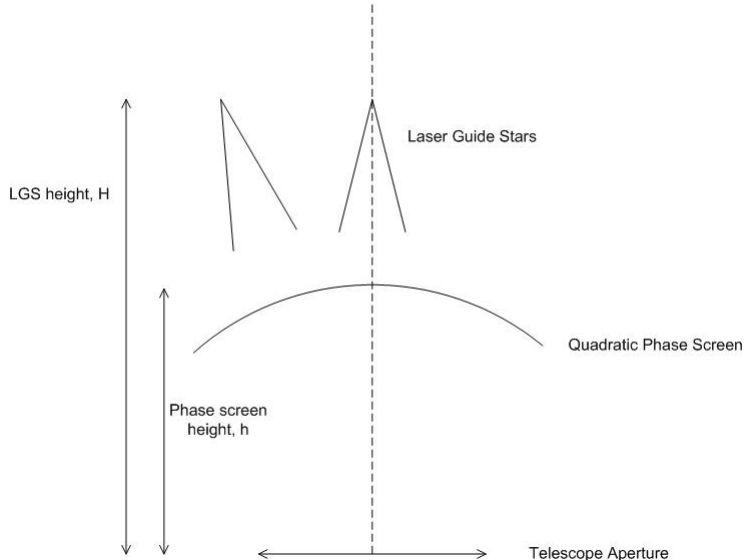
Figure 1: Illustration of the toy problem – schematic of a one-dimensional phase screen, and sensing with multiple LGS.

order or higher cancel out when probed by the LGS, leaving only constant and linear terms (i.e. piston and tip/tilt) in each LGS beam, resulting in a null measurement when TT is filtered. In theory, an infinite number of these modes exist, but by virtue of the steep slope of the Kolmogorov power spectrum, most of the power is contained within the first few low-order null-modes created by combinations of quadratic and cubic modes. How many of these tilt anisoplanatism null-modes one wants to measure and correct will determine how many measurements the NGS are required to provide. To correct up to second-order null-modes, only three TT NGS are required. For third-order null-modes, more TT NGS or a combination of TT NGS and TT+focus+astigmatism (TTFA) NGS are required.

The quadratic tomography error of item (2) is expected to be smaller than the tilt anisoplanatism and essentially field-independent, but it can contribute a substantial error on-axis if not corrected for. The error comes about as in the special case of quadratic modes, no more information is obtained by employing multiple LGS beacons than is given by a single LGS, and hence the cone effect persists for these three modes. The solution is again to invoke more and/or higher-order measurements from NGS. A NGS-based null-mode compensation system designed to compensate *at least* the quadratic tilt anisoplanatism null-modes, will automatically also include correction of the quadratic tomography error. However, the main point that is stressed here is that even if one does not require multiple or quadratic NGS for tilt anisoplanatism correction off-axis (in e.g. an on-axis science case), this fidelity of NGS measurements is still needed for correcting the quadratic tomography error on-axis.

1.2 A toy problem

This toy problem is an extreme simplification only to illustrate some of the effects involved. This is an old analysis in a slightly modified context. The original discussion is given by Ellerbroek and Rigaut[2]. See some of the same information in Lloyd-Hart and Milton[5].

Consider one dimensional telescope, coordinates in the aperture are x. The vertical extent of the atmosphere is described by coordinate h. The atmosphere is composed of only a single thin phase screen at distance, h, above the telescope aperture, see Fig. 1 for a diagram. The screen is assumed to only contain a focus aberration described by

$$s = ax^2. \tag{1}$$

In all that follows we assume geometrical optics, and use the standard summation over phase screens for propagation through the atmosphere. For an NGS source on axis the wavefront phase measured at the aperture will be

$$\varphi_n(0) = s(x) = ax^2. \tag{2}$$

Similarly for an off-axis source, denoted by, θ, the wavefront phase at the aperture will be

$$\varphi_n(\theta) = s(x + h\theta) = a(x^2 + 2xh\theta + h^2\theta^2). \tag{3}$$

2

The last term in the expansion is a constant (piston) term in the wavefront and is not usually measured (I do not consider interferometry). The term linear in x is a tilt term, as I move off axis the amount of tilt in the wavefront increases. The x^2 term is a focus error. Now consider probing this screen with an on-axis LGS that samples the phase screen with an expanding spherical wavefront. The height of the laser is H. Replace x by $x\gamma_h$ where $\gamma_h = 1 - h/H$.

$$\varphi_l(0) = s(x\gamma_h) = ax^2\gamma_h^2. \tag{4}$$

To summarize, for a conventional single LGS system with both the science target and LGS on-axis the two measured wavefronts are

$$\varphi_n(0) = ax^2, \tag{5}$$
$$\varphi_l(0) = ax^2\gamma_h^2 = ax^2\left(1 - \frac{h}{H}\right)^2. \tag{6}$$

The difference between the wavefronts is just the usual single LGS focus anisoplanatism term, note that if the phase screen altitude goes to zero, $h = 0$, or the LGS altitude H goes to infinity, then the two wavefronts are identical and no wavefront error results. In order to make a perfect estimate of the wavefront one needs to know both a and h, which is impossible with a single LGS.

Next consider attempting to minimize focus anisoplanatism by adding in more LGS slightly off axis, these LGS positions will be denoted by θ_i, for the ith LGS. For a LGS beam located off-axis replace x with $x\gamma_h + h\theta_i$, and the resulting measurement from the laser guide star is

$$\varphi_l(\theta_i) = s(x\gamma_h + h\theta_i) = a\left(x^2\gamma_h^2 + 2x\gamma_h h\theta_i + h^2\theta_i^2\right). \tag{7}$$

Like the NGS case the piston term is not important and is filtered out. The term that is proportional to x is a tilt term; this cannot be sensed by conventional LGS because of position uncertainty in the LGS. We filter these terms out resulting in the surprising result that

$$\varphi_l(\theta_i) = ax^2\left(1 - \frac{h}{H}\right)^2. \tag{8}$$

It appears that off axis LGS give no new information about the focus error in the phase screen, adding more LGS does not improve your measurement. Note this is only a problem for x^2 type aberrations. If the phase screen contained a pure cubic aberration (x^3) then

$$\varphi_n(\theta) = a(x + h\theta)^3 = a(x^3 + 3x^2h\theta + 3xh^2\theta^2 + h^3\theta^3) \tag{9}$$
$$\varphi_l(\theta_i) = a(x\gamma_h + h\theta_i)^3 = a(x^3\gamma_h^3 + 3x^2\gamma_h^2 h\theta_i + 3x\gamma_h h^2\theta_i^2 + h^3\theta_i^3). \tag{10}$$

Dropping tilt terms (just LGS) and piston (NGS and LGS) terms, the result is

$$\varphi_n(\theta) = a(x^3 + 3x^2h\theta + 3xh^2\theta^2) \tag{11}$$
$$\varphi_l(\theta_i) = a(x^3\gamma_h^3 + 3x^2\gamma_h^2 h\theta_i). \tag{12}$$

In this case adding more LGS does provide new information and a clever tomography algorithm should be able to improve the wavefront estimate with more LGS. It is important to note that the problems arise from the lack of tilt information provided by LGS. I have not invoked anything more complicated. Specifically this discussion does not depend on the details of MCAO, MOAO, LTAO, or the specifics of the tomography algorithm.

1.2.1 Discussion

The problem can be eliminated by one of the following techniques, at least in the simple 1-d problem:

1. Use the on-axis science target to measure the quadratic terms directly, i.e. measure focus with the NGS.

2. Use (at least) three off-axis TT NGS to measure tilt in multiple directions, estimate quadratic terms and height of phase screens.

3. Use a LGS at a different height H, say a Rayleigh beacon, and use the two LGS to estimate quadratic terms and height of phase screens.

4. Use a MASS/DIMM to measure h directly (possible in the toy problem; probably not in reality)

5. Ignore the problem if it is a small correction factor (unfortunately not always the case, see Sect. 4)

In the toy problem you have two unknowns: a the phase screen strength and h the distance to the phase screen. In a real atmosphere you don't have a single phase screen with just a focus aberration however the focus component in the upper atmosphere will be measured incorrectly by a laser guide star. In the single LGS case this error is just lumped into the focus anisoplanatism term in the error budget. A modal decomposition of this error term, reveals that focus, and the two astigmatisms are the dominate terms, see e.g. Esposito et al. 1996[3].

2 Tomography error analysis

What follows is a modal tomography approach to estimating the residual wavefront error from LGS null-modes in a combined LGS+NGS tomography AO system. The methodology is in principle equivalent to that given in [1], but the transformation matrices are here calculated by geometric integration in a numerical simulation instead of via analytical formulas based on monomial transformations.

2.1 System type and corrector geometry

To forestall confusion on this point, it is addressed here what it implies for the analysis if the AO system is operating in multi-conjugate (MCAO) mode, multi-object (MOAO) mode, or in laser tomography (LTAO) mode. As always with wavefront reconstruction in tomographic AO systems, the two steps of wavefront estimation and correction can be separated. The first step entailing wavefront estimation depends only on the geometry of NGS and LGS and the number of modes measured, and not at all on the specific type of AO operation. The difference comes in at the point of applying the estimated correction. In terms of correction strategy, both MCAO and MOAO employ a combination of at least 2 DMs to implement the null-mode correction for a given position in the field of view, while LTAO uses only one DM. This means that LTAO can strictly only be "correct" for a single point in the field (e.g. on-axis), while MCAO and MOAO can be optimized for multiple field positions simultaneously. Both MCAO and LTAO however have the option to have their null-mode correction optimized for an extended and contiguous field of view rather than preferentially for discrete field points. Thus, the second difference comes in at the point of computing the null-mode wavefront estimator, where for MOAO you must always compute a separate estimator for each science object; for LTAO you must choose either a single direction to optimize for or else a field of view to average over; and for MCAO you can either do nothing at all and it will optimize performance for the NGS positions, or you can supply it with other field points to optimize for and average over. All the cases that imply averaging and/or optimizing for field points other than the NGS will require the use of a Bayesian type estimator like e.g. the minimum variance estimator (MVE). By using a purely geometrical least-squares estimator (referred to as SVD, for singular value decomposition), the analysis of the next section is equivalent to the MCAO "do-nothing" case that simply optimizes for the NGS positions.

2.2 Null-mode estimation

Denote by φ_ε the residual phase error at the pupil plane integrated along one given direction (we omit the angle variable for brevity, and keep in mind that each matrix or vector will have a separate block for each guide star or evaluation position):

$$\varphi_\varepsilon = \varphi - \widehat{\varphi}, \tag{13}$$

where φ is the atmospheric turbulence and $\widehat{\varphi}$ the correction applied by the AO system, both quantities integrated down to the pupil plane along the same cylindrical beam. We describe the two-dimensional phase by a Zernike expansion

$$\varphi_\varepsilon(\rho, \theta) = \sum_{i=2}^{N} \varepsilon_i Z_i(\rho/R, \theta) = Z\varepsilon,$$

where ε is the vector of residual Zernike coefficients at the telescope pupil of radius R. The latter matrix algebra formulation is the one that we will adopt from now on, with upper-case letters denoting matrices and lower-case denoting vectors. We then have that $\varphi = Za$ and $\widehat{\varphi} = Z\widehat{a}$, where a and $\widehat{a}$ are the Zernike coefficient vectors of the input atmospheric turbulence and the reconstructed modes. The residual error can be written as

$$\varepsilon = P_a a - P_m \widehat{a},$$

where P_a and P_m are projection matrices that integrate the modal content through all turbulent layers (P_a) and DMs (P_m) on-axis. a has the length $N_z N_l$ where N_z is the number of Zernike modes and N_l is the number of turbulence layers; $\widehat{a}$ has the length $N_z N_m$, where N_m is the number of DMs. The AO system mode sensing and reconstruction in open loop is done as follows:

$$
\begin{align}
\widehat{a} &= Em, \tag{14}\\
m &= Ga, \tag{15}
\end{align}
$$

where G and E are, respectively, the (combined LGS and NGS) measurement and reconstruction operators acting on the input turbulence mode a and the resulting measurement vector m. E is in this analysis obtained from a SVD inversion of the modal interaction matrix G, where a varying number of null-modes may be filtered in the inversion, depending on the geometry. Putting it together we obtain

$$\varepsilon = (P_a - P_m EG)a = Qa$$

where $Q = P_a - P_m EG$ is an operator that depends only on the geometry of the system (LGS and NGS positions and altitudes, DM and turbulence layer altitudes) and the evaluation direction. The variance of the residual phase error is then

$$
\begin{align}
\sigma_\varepsilon^2 &= \langle \varphi_\varepsilon^T \varphi_\varepsilon \rangle = \mathrm{Tr}\left[\langle \varphi_\varepsilon \varphi_\varepsilon^T \rangle\right] = \mathrm{Tr}\left[Z \langle \varepsilon \varepsilon^T \rangle Z^T\right] \tag{16}\\
&= \mathrm{Tr}\left[ZQ\langle aa^T \rangle Q^T Z^T\right] = \mathrm{Tr}\left(QC_a Q^T\right), \tag{17}
\end{align}
$$

where $\mathrm{Tr}()$ denotes the trace operation, and we exploited the invariance of the trace under a similarity transform $\mathrm{Tr}(BAB^{-1}) = \mathrm{Tr}(A)$, since $Z^T = Z^{-1}$ by orthogonality of the Zernike modes. $C_a = \langle aa^T \rangle$ is the covariance matrix of Zernike coefficients, which can be computed for Kolmogorv (Noll, 1976; Wang & Markey 1978)[6, 7] or von Karman (Winker, 1991)[8] statistics. For low-order modes and a large aperture, von Karman statistics should be used. The Q matrix can be computed from straightforward geometric considerations and the trace (17) evaluated, which is done in the next section. If WFS noise is included we modify equation (15) according to

$$m = Ga + Tn, \tag{18}$$

where n is the noise on the WFS measurement and T a transformation that propagates WFS noise onto Zernike modes. T can be modeled for a given WFS type and architecture – the Shack-Hartmann type was used in this case. It is straightforward to evaluate the new expression which simply acquires an additional term

$$\sigma_\varepsilon^2 = \mathrm{Tr}\left(QC_a Q^T\right) + \mathrm{Tr}\left(SC_n S^T\right), \tag{19}$$

where $S = P_m ET$ and $C_n = \langle nn^T \rangle$ is the noise covariance matrix. These two terms can be computed separately to study the residual null-mode error due to purely geometric constraints and due to noise propagation. The presence of noise can also be included in E by choosing a noise-weighted (Gauss-Markov) or minimum variance type estimator.

3   Sample numerical results

A numerical simulation was set up with an atmospheric model consisting of 7 layers (the Neyman CN-M3 Mauna Kea model), and a baseline MCAO system with 5 LGSs in a quincunx asterism of $11''$ radius. The parameters that varied between the configurations were:

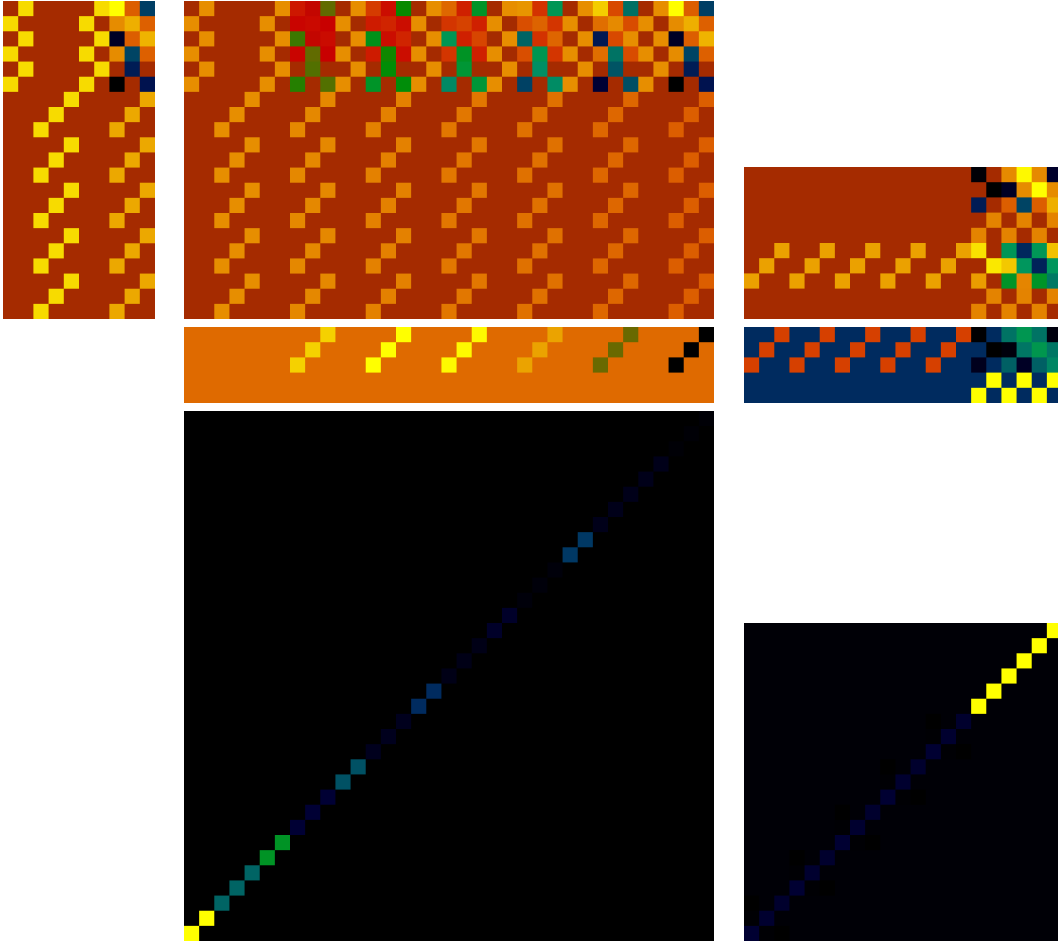- maximum radial order of atmospheric modes (2 or 3)

- number of NGS (1 or 3)

Figure 2: The usual suspects. From left to right, top to bottom: G_m, G_a, E_m, $Q(0)$, $S(0)$, C_a and C_n.

- maximum radial order of NGS (1 or 2)

- number of wavefront estimator layers (2 or 3)

- number of filtered null-modes

Noise was included in the simulations not with an aim to make absolute statements about the limiting magnitudes, but merely for indicating the general effect of having noise in the system. The rudimentary noise modeling used a 15 magnitude (J band) NGS. Some sample numerical results are presented in Sect. 4.

4 Anatomy of a null-mode

4.1 Quadratic atmosphere/LGS, 2 estimator layers

4.1.1 Case #1: 1 TT NGS $0''$, 10 modes, 5 null

```
On-axis error (tomo/noise) per mode (nm RMS):
   0.000    0.000   28.209   28.209   28.209
  10.123   10.123    0.023    0.022    0.022
On-axis error (tomo/noise) per radial order (nm RMS):
   0.000   48.860
  14.316    0.038
```

4.1.2 Case #2: 3 TT NGS $40''$, 10 modes, 2 null

```
On-axis error (tomo/noise) per mode (nm RMS):
   0.000   0.000   0.631   0.631   0.631
   5.844   5.844   0.914   1.308   1.275
On-axis error (tomo/noise) per radial order (nm RMS):
   0.001   1.094
   8.265   2.043
```

4.2 Cubic atmosphere/LGS, 2 estimator layers

4.2.1 Case #3: 3 TT NGS $40''$, 18 modes, 4 null

```
On-axis error (tomo/noise) per mode (nm RMS):
  30.194  30.201   3.778   3.444   3.362   6.287   6.281   5.767   1.449
   6.175   6.175   0.913   1.292   1.260   0.103   0.091   1.698   0.039
On-axis error (tomo/noise) per radial order (nm RMS):
  42.706   6.118  10.693
   8.733   2.022   1.704
```

4.2.2 Case #4: 3 TT NGS $40''$, 18 modes, 2 null

```
On-axis error (tomo/noise) per mode (nm RMS):
  16.222  16.264   3.777   1.935   1.915   0.419   0.411   5.771   1.448
   5.845   5.846   0.913   1.308   1.274   0.038   0.038   1.697   0.039
On-axis error (tomo/noise) per radial order (nm RMS):
  22.971   4.656   5.979
   8.266   2.042   1.699
```

4.2.3 Case #5: 3 TTFA NGS $40''$, 18 modes, 2 null

```
On-axis error (tomo/noise) per mode (nm RMS):
  13.171  13.204   1.920   0.979   0.974   0.313   0.309   2.418   1.130
   6.083   6.083   1.147   1.438   1.476   0.392   0.393   0.677   0.604
On-axis error (tomo/noise) per radial order (nm RMS):
  18.650   2.365   2.705
   8.603   2.359   1.064
```

4.3 Cubic atmosphere/LGS, 3 estimator layers

4.3.1 Case #6: 3 TTFA NGS $40''$, 27 modes, 11 null

```
On-axis error (tomo/noise) per mode (nm RMS):
   9.254   9.284   1.905   0.735   0.732   0.233   0.223   1.847   1.097
   5.973   5.974   1.144   1.435   1.473   0.398   0.399   0.605   0.599
On-axis error (tomo/noise) per radial order (nm RMS):
  13.108   2.169   2.173
   8.448   2.353   1.021
```

4.3.2 Case #7: 3 TTFA NGS $40''$, 27 modes, 7 null

```
On-axis error (tomo/noise) per mode (nm RMS):
   1.842   1.816   0.271   0.260   0.263   0.060   0.060   0.702   0.704
  12.917  12.600   1.605   1.913   1.982   0.342   0.346   0.688   0.541
On-axis error (tomo/noise) per radial order (nm RMS):
   2.586   0.458   0.998
  18.045   3.188   1.001
```
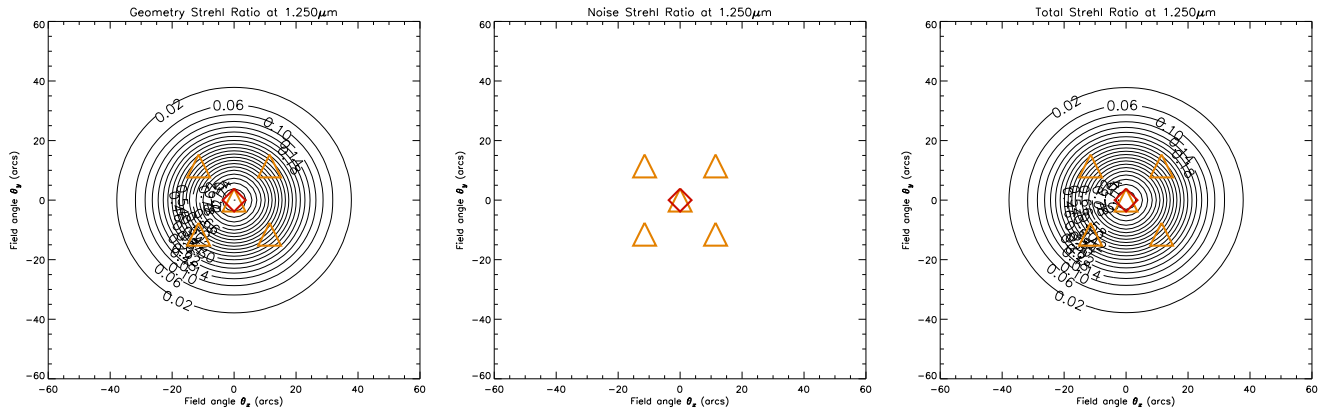
Figure 3: Case #1: Quadratic atmosphere/LGS, 2 estimator layers, 1 TT NGS $0''$: 10 modes, 5 null.
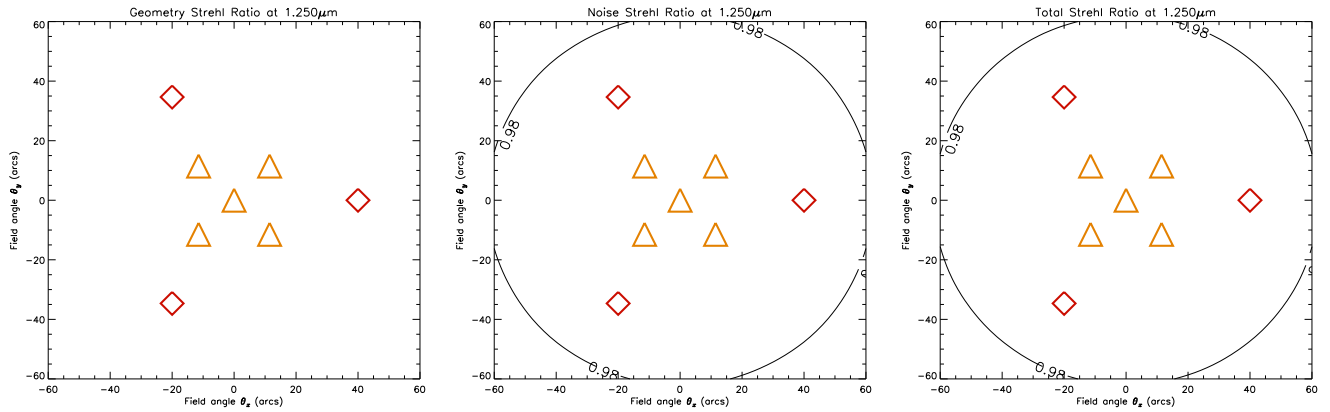

Figure 4: Case #2: Quadratic atmosphere/LGS, 2 estimator layers, 1 TT NGS $40''$: 10 modes, 2 null.

4.3.3 Case #8: 3 TTFA NGS $40''$, 27 modes, 4 null

```
On-axis error (tomo/noise) per mode (nm RMS):
   0.510    0.430    0.006    0.007    0.007    0.049    0.049    0.701    0.701
  10.981   10.943    2.522    2.993    3.145    0.234    0.236    0.675    0.410
On-axis error (tomo/noise) per radial order (nm RMS):
   0.668    0.012    0.994
  15.502    5.020    0.857
```

References

[1] R. M. Clare and B. L. Ellerbroek. Sky coverage estimates for adaptive optics systems from computations in Zernike space. *J. Opt. Soc. Am. A*, 23:418–426, February 2006.

[2] Brent L. Ellerbroek and François Rigaut. Methods for correcting tilt anisoplanatism in laser-guide-star-based multiconjugate adaptive optics. *J. Opt. Soc. Am. A*, 18(10):2539–2547, October 2001.

[3] S. Esposito, A. Riccardi, and R. Ragazzoni. Focus anisoplanatism effects on tiptilt compensation for adaptive optics with use of a sodium laser beacon as a tracking reference. *J. Opt. Soc. Am. A*, 13:1916–1923, September 1996.
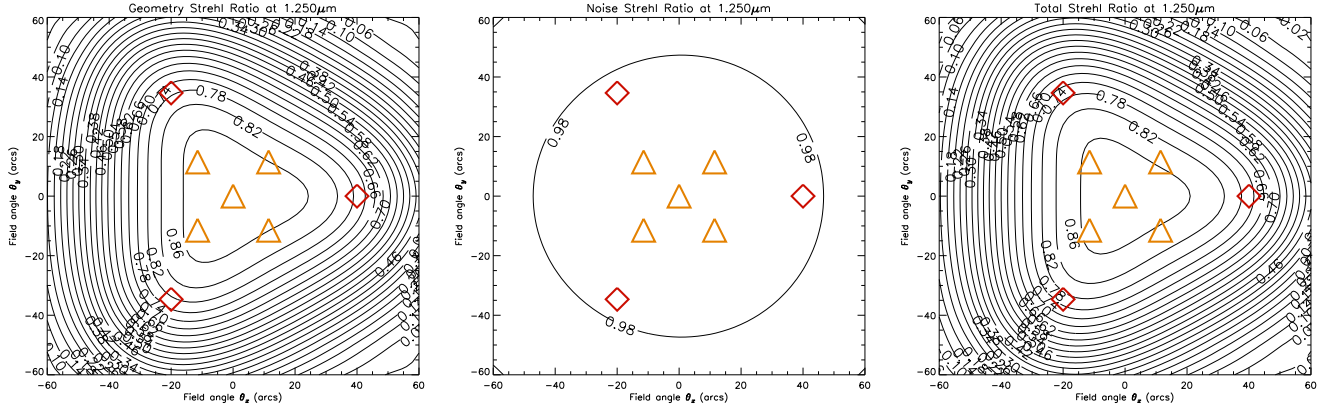
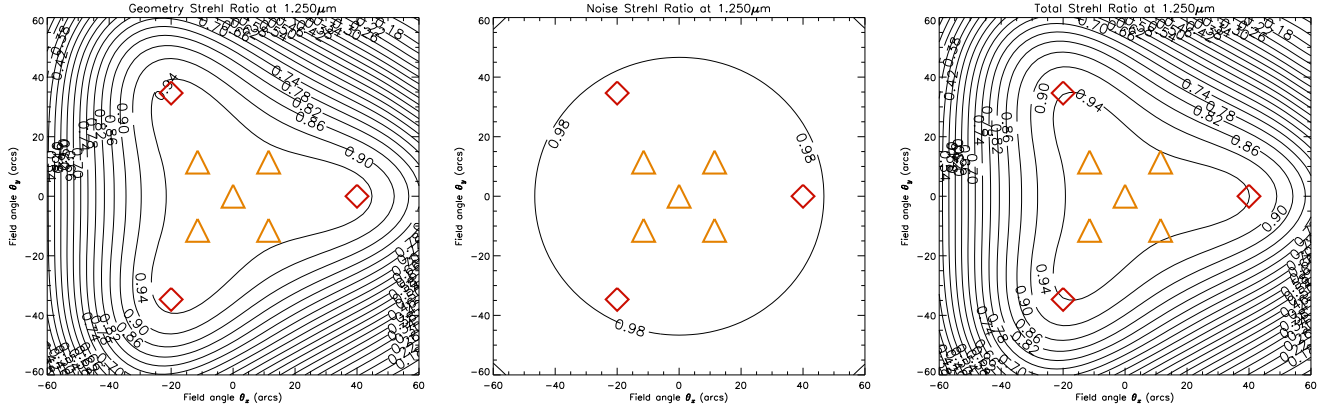Figure 5: Case #3: Cubic atmosphere/LGS, 2 estimator layers, 3 TT NGS 40″: 18 modes, 4 null.

Figure 6: Case #4: Cubic atmosphere/LGS, 2 estimator layers, 3 TT NGS 40″: 18 modes, 2 null.

[4] R. C. Flicker, F. J. Rigaut, and B. L. Ellerbroek. Tilt anisoplanatism in laser-guide-star-based multiconjugate adaptive optics. Reconstruction of the long exposure point spread function from control loop data. *Astron. Astrophys.*, 400:1199–1207, March 2003.

[5] M. Lloyd-Hart and N. M. Milton. Fundamental limits on isoplanatic correction with multiconjugate adaptive optics. *J. Opt. Soc. Am. A*, 20:1949–1957, October 2003.

[6] R. J. Noll. Zernike polynomials and atmospheric turbulence. *J. Opt. Soc. Am.*, 66(3):207–211, 1976.

[7] J. Y. Wang and J. K. Markey. Modal compensation of atmospheric turbulence phase distortion. *J. Opt. Soc. Am.*, 68(1):78–87, 1978.

[8] D. M. Winker. Effect of a finite outer scale on the Zernike decomposition of atmospheric optical turbulence. *J. Opt. Soc. Am. A*, 8(10):1568–1573, 1991.
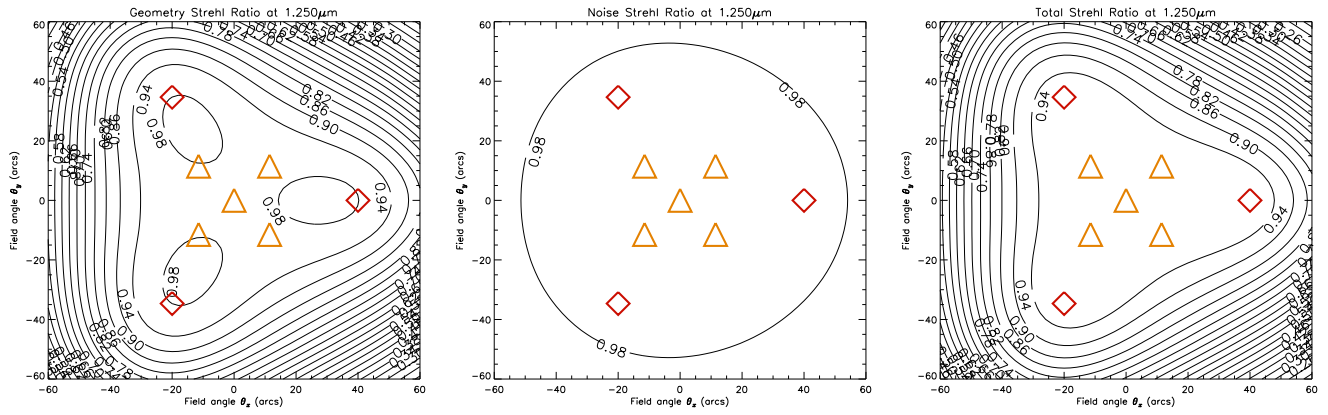
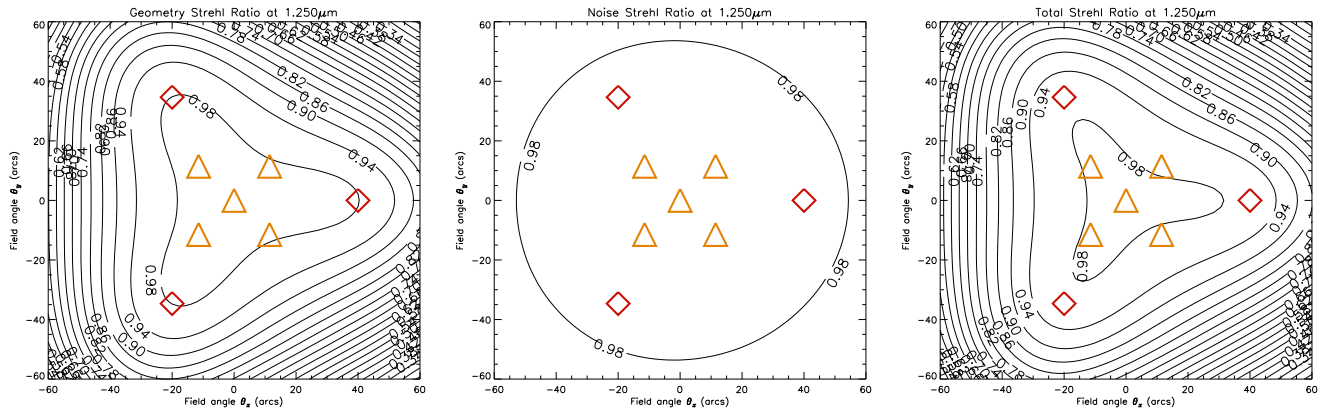Figure 7: Case #5: Cubic atmosphere/LGS, 2 estimator layers, 3 TTFA NGS 40″: 18 modes, 2 null.

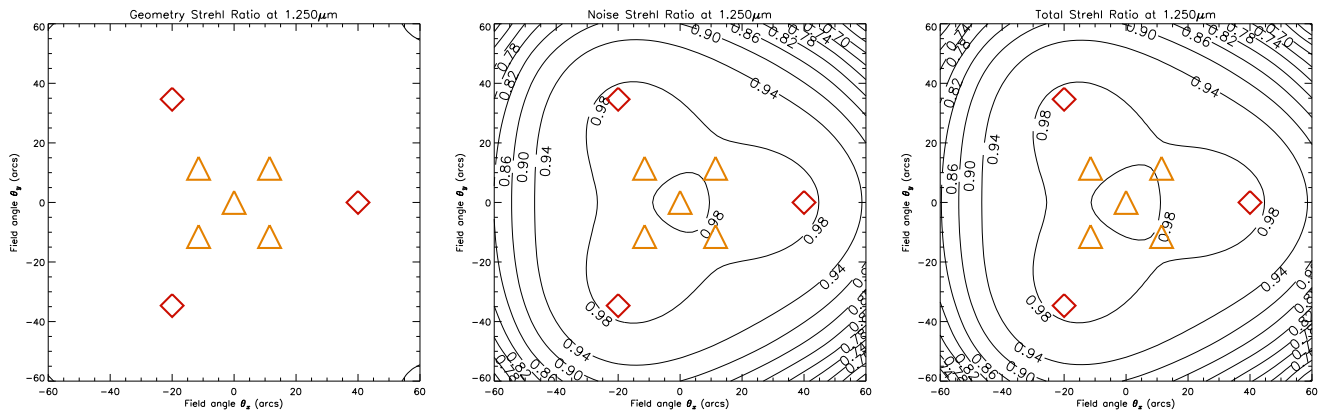Figure 8: Case #6: Cubic atmosphere/LGS, 3 estimator layers, 3 TTFA NGS 40″: 27 modes, 11 null.

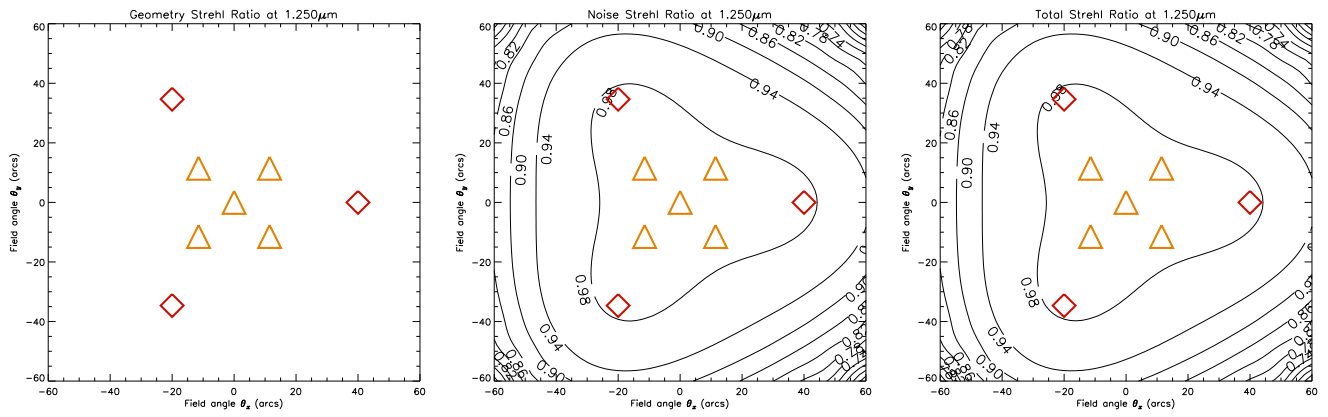Figure 9: Case #7: Cubic atmosphere/LGS, 3 estimator layers, 3 TTFA NGS 40″: 27 modes, 7 null.

10

Figure 10: Case #8: Cubic atmosphere/LGS, 3 estimator layers, 3 TTFA NGS 40″: 27 modes,4 null.
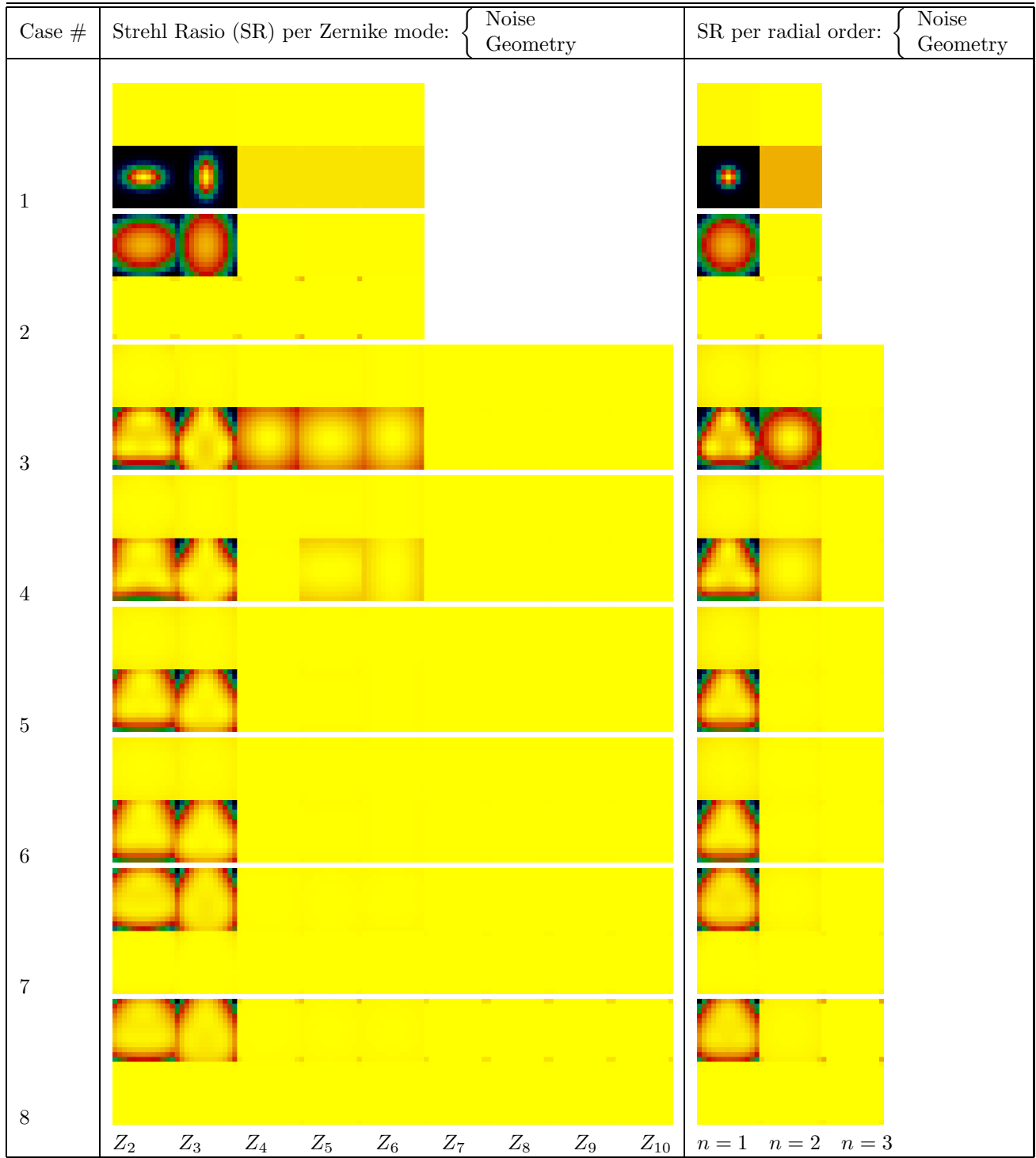
Figure 11: Strehl maps (over the field of view) per mode and radial order for each simulated configuration.